Supplementary information

In-situ biomass-confined construction of atomical Fe/NC catalyst towards oxygen reduction reaction

Mingfu Ye,[a,b,c] Yang Li,[a] Jieyue Wang,[a] Linxiao Zhan,[a] Mingyue Wang,[a] Chunsheng Li,[c] Wenhai Wang,*[a,c] Guohong Fan,*[b] Chang Chen*[d] and Konglin Wu*[a,e]

[a] Institute of Clean Energy and Advanced Nanocatalysis (iClean), School of Chemistry and Chemical Engineering, Anhui University of Technology, Maanshan 243032, China

[b] Engineering Research Center of Biofilm Water Purification and Utilization Technology of Ministry of Education, Anhui University of Technology, Maanshan 243032, China

[c] Key Laboratory of Advanced Electrode Materials for Novel Solar Cells for Petroleum and Chemical Industry of China, School of Chemistry and Life Sciences, Suzhou University of Science and Technology, Suzhou, 215009, China

[d] Engineering Research Center of Advanced Rare Earth Materials, Department of Chemistry, Tsinghua University, Beijing 100084, China

[e] State Key Laboratory of Heavy Oil Processing, China University of Petroleum (East China), Qingdao 266580, China

E-mail: wenhaiwang@ahut.edu.cn (W. Wang); ghfan8@ahut.edu.cn (G. Fan); changchencc@yeah.net (C. Chen); klwuchem@ahut.edu.cn (K. Wu)

Experimental

Chemicals

Iron chloride hexahydrate ($FeCl_3 \cdot 6H_2O$, 99%, Sinopharm); Chitosan ($(C_6H_{11}NO_4)_n$, 99%, Adamas); Spherical silica (SiO_2, diameter: 50 nm, 99%, Macklin); Melamine ($C_3H_6N_6$, 99%, Alfa); Acetic acid ($C_2H_4O_2$, 99.5%, Sinopharm Chemical Reagent Co., Ltd); Ethanol (C_2H_5OH, 99%, Sinopharm); Water (H_2O, Wahaha Group Co., Ltd); Nafion (D-521 dispersion, 5% w/wt in water and 1-propanol, >0.92 meq/g exchange capacity, Alfa), Ammonium bifluoride (NH_4HF_2, 95%, Macklin).

Preparation of catalysts

Synthesis of Fe/NC:

2 g chitosan, 2 g melamine and 2 g SiO_2 were dispersed in 50 mL water. Then 100 mg $FeCl_3 \cdot 6H_2O$ and 0.5 mL acetic acid were introduced in the above dispersion. The sample was stirred at 70 ℃ for 5 h to generate the Fe(III)-chitosan hydrogel, followed by freeze-drying. The dried sample was firstly pyrolyzed in an N_2 atmosphere at 550 ℃ for 2 h (ramp: 2 ℃ min^{-1}) and then pyrolyzed under a flow of N_2 at 900℃ for 3 h (ramp: 2 ℃ min^{-1}). The synthetic product was immersed in 4 M NH_4HF_2 for 12 h at 70 ℃ to remove SiO_2 template and then the product was respectively washed by water and ethanol. Fe/NC was finally obtained by being dried in an oven at 50 °C overnight.

Synthesis of NC:

NC was prepared by the same procedures as Fe/NC. The difference is that there is no involved $FeCl_3 \cdot 6H_2O$.

Characterization

The crystal structures of catalyst were characterized with X-ray powder diffraction (XRD, Rigaku Ultima IV). Transmission electron microscopy (TEM, Hitachi HT 7700 type) was used to investigate the morphologies of catalysts. Aberration-corrected high-angle annular dark-field scanning transmission electron microscopy (HAADF-STEM) was implemented by a field emission electron microscopy (JEOL, JEM-2100F, operating voltage: 200 kV). The chemical composition analysis was carried out by ICP-OES (PE Avio200). Raman spectra were acquired from a laser confocal Raman spectrometer (Renishaw, InVia). N_2 adsorption/desorption measurements were carried out by Micromeritics ASAP 2460. X-ray photoelectron spectroscopy (XPS) was taken by PHI Quantera SXM equipment. The Fe K-edge X-ray absorption fine structure (XAFS) spectra of Fe/NC was obtained at Beijing Synchrotron Radiation Facility (BSRF, operating voltage: 2.5 GeV). Utilizing the ATHENA module of the IFEFFIT software packages, the obtained EXAFS data were performed according to the standard procedures.[1] The EXAFS contributions were separated from different coordination shells by using a hanning windows. Subsequently, the quantitative curve-fittings were carried out in the R-space with a Fourier transform k-space range using the module ARTEMIS of IFEFFIT. During the curve-fitting, the overall amplitude reduction factor S_0^2 was fixed to the best-fit value determined from fitting the data of metal foil. For the sample, the structural parameters, such as the coordination number N, interatomic distance R, the Debye-Waller factor σ^2 and the edge-energy shift ΔE_0 were allowed to vary during the fitting process.

Electrochemical measurements

The ORR activities of catalysts were explored in a three-electrode system by a CHI 760E electrochemical workstation. The glassy carbon electrode, Ag/AgCl and graphite rod were individually employed as the working electrode, reference electrode and counter electrode. The catalyst ink was composed of 5 mg catalyst, 500 μL water, 450 μL ethanol and 50 μL Nafion. After sonicating for 30 min, 20 μL catalyst ink was dropped on rotating disk electrodes (RDE, diameter: 5 mm) or rotating ring-disk electrodes (RRDE, diameter: 5.6 mm). All measured potentials (V *vs* Ag/AgCl) were converted to reversible hydrogen electrode (RHE) potentials according to the equation below:

$$E_{RHE}=E_{Ag/AgCl}+0.197+0.059pH \quad (1)$$

Cyclic voltammetry (CV) was performed in O_2-saturated or N_2-saturated 0.1 M KOH solution with a scan rate of 10 mV s^{-1}. Linear scanning voltammetry (LSV) was executed in O_2-saturated 0.1 M KOH at 1600 rpm with a scan rate of 5 mV s^{-1}. The methanol tolerance of catalysts was investigated by adding 2.0 mL methanol into the 0.1 M KOH electrolyte (98 mL). The ORR durability of catalysts was assessed by an accelerated durability test (ADT), where catalysts were cycled 4000 times at 0.6-1.0 V under an O_2-saturated 0.1 M KOH electrolyte.

RRDE was utilized to measure the electron transfer number (n) and hydrogen peroxide yield ($\%H_2O_2$) during the ORR and these related values were calculated based on the following equations:

$$n=4\times I_d/(I_r/N+I_d) \quad (2)$$

$$\%H_2O_2=200I_r/N/(I_r/N+ I_d) \quad (3)$$

where the collection efficiency N is 0.37, I_d is the disk current and I_r is the ring current.

2.5 Zn-air battery measurements:

The homemade liquid ZAB was assembled with catalysts-coated carbon paper as the air cathode, Zn foil as the anode and 6 M KOH+0.2 M $Zn(CH_3COO)_2$ as the electrolyte. The catalyst ink of air cathodes was proceeded with in the same way as that of catalyst-coated glassy carbon electrodes. The catalyst ink was dropped on carbon paper and the corresponding catalyst loading is 0.4 mg cm^{-2}. The polarization curves of homemade liquid ZABs were performed on a CHI 760E electrochemical workstation and the power density plots were derived from the polarization curves. The cycling measurements of homemade liquid ZABs were implemented with a Neware battery testing system (CT-4008Tn). One cycle consisted of 5 min for discharging and 5 min for charging.

The coin-type ZAB was constructed with catalysts-coated carbon paper (catalyst loading: 0.4 mg cm^{-2}) as the air cathode, Zn foil as the anode, glass fiber paper as the separator and 6 M KOH+0.2 M $Zn(CH_3COO)_2$ as the electrolyte. The cycling stability of coin-type ZAB was also recorded with a Neware battery testing station system (CT-4008Tn).

Theoretical calculation

The DFT calculations were performed using the DMol3 module of the Materials studio software.[2, 3] The Generalized-Gradient-Approximation (GGA) and Perdew-Burke-Ernzerhof (PBE) were used to describe the exchange-correlation functional. The Grimme method was used to correct van der Waals (vdW) interactions in all

calculations.[4] Double-numerical plus polarization (DNP)[5] is used as the atomic orbital basis set to describe the wave function of valence electrons. The threshold of energy and force were 1.0×10^{-5} Ha and 2.0×10^{-3} Ha·Å^{-1}. The cutoff radius of the atomic orbital in real space was set as 5.0 Å. A 2 × 2 × 1 Monkhorst-Pack k-point brillouin zone sampling was chosen for the geometry optimization. A vacuum distance of 20 Å in the z-direction was used to prevent interactions between adjacent layers. The conductor-like shielding model (COSMO) was used to simulate the aqueous solvent environment with the dielectric constant set to 78.54.

References

1. M. Newville, *J. Synchrotron Radiat.* 2001, **8**, 322-324

2. B. Delley, *J. Chem. Phys*. 1990, **92**, 508-517.

3. B. Delley, *J. Chem. Phys.* 2000, **113**, 7756-7764.

4. S. Grimm, J. Antony, S. Ehrlich and H. Krieg, *J. Chem. Phys.* 2010, **132**, 154104.

5. P. Liu and J. A. Rodriguez, *J. Am. Chem. Soc.* 2005, **127**, 14871-14878.

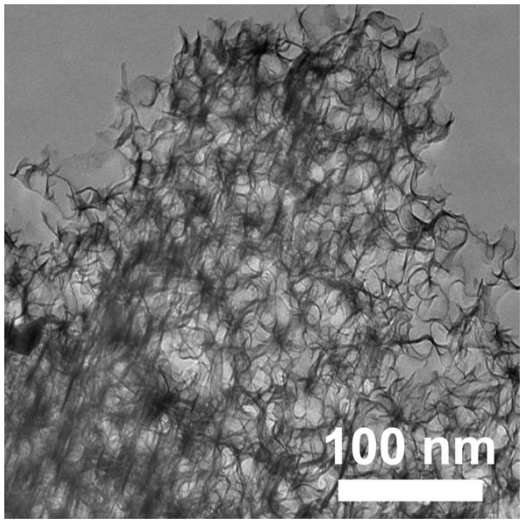

Fig. S1 TEM image of NC.

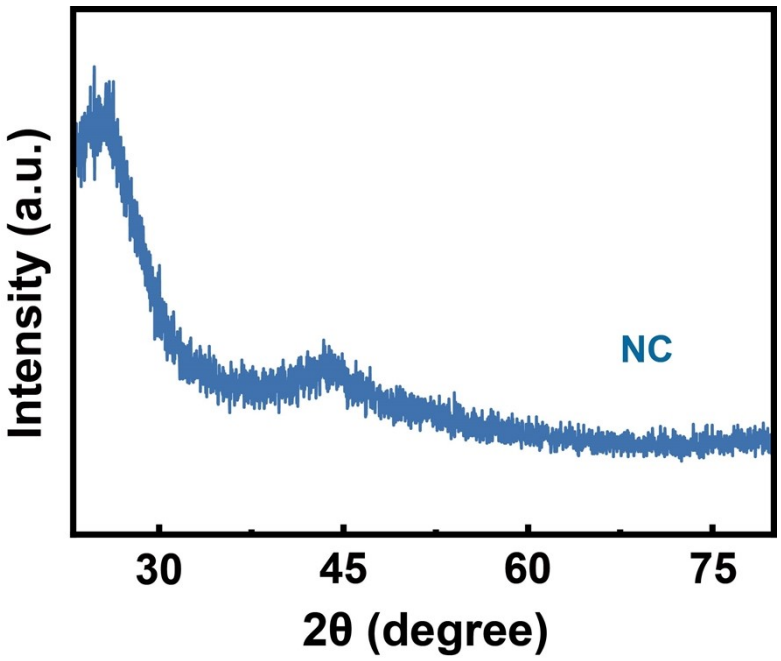

Fig. S2 XRD patterns of NC.

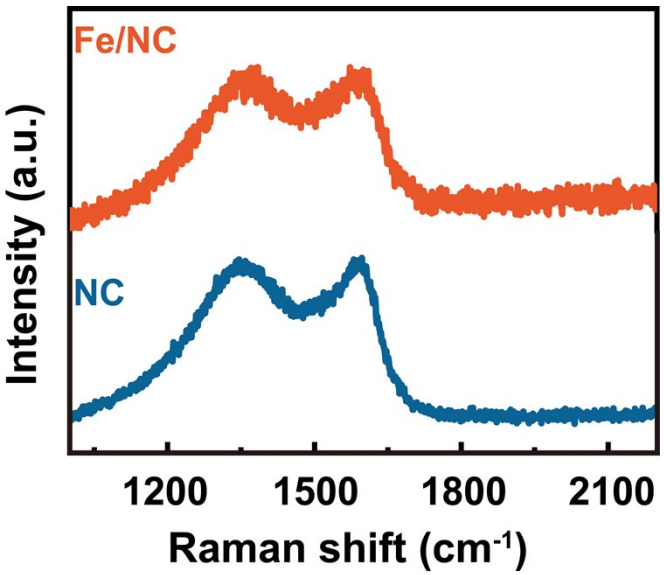

Fig. S3 Raman spectra of catalysts.

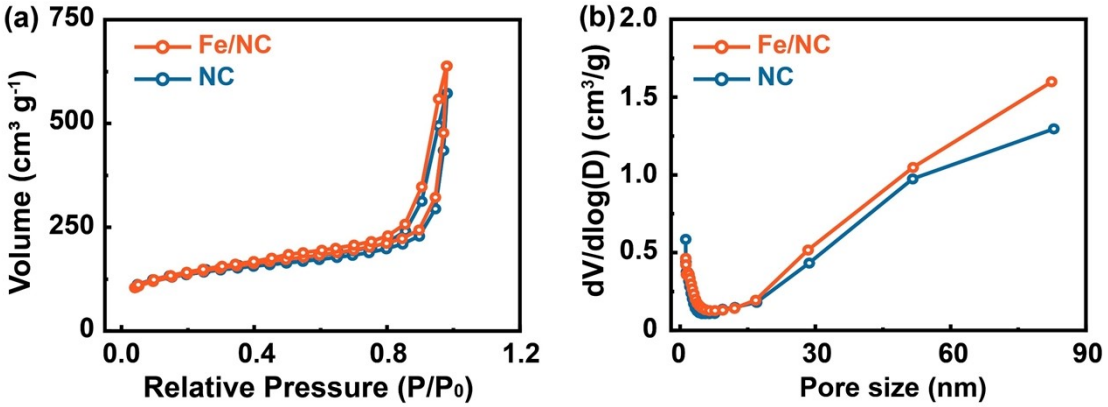

Fig. S4 (a) N_2 adsorption/desorption isotherm curves of catalysts. (b) Pore size distribution curve of catalysts.

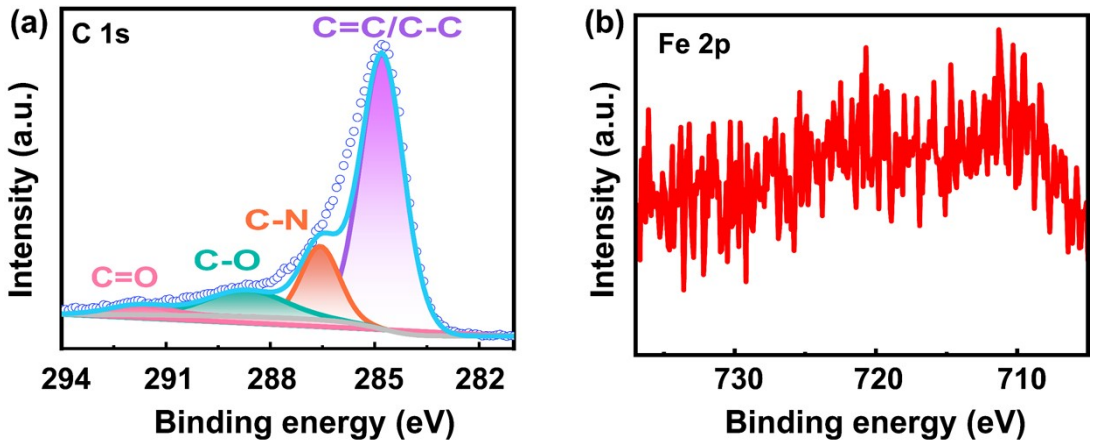

Fig. S5 XPS spectra of Fe/NC: (a) C 1s spectra. (b) Fe 2p spectra.

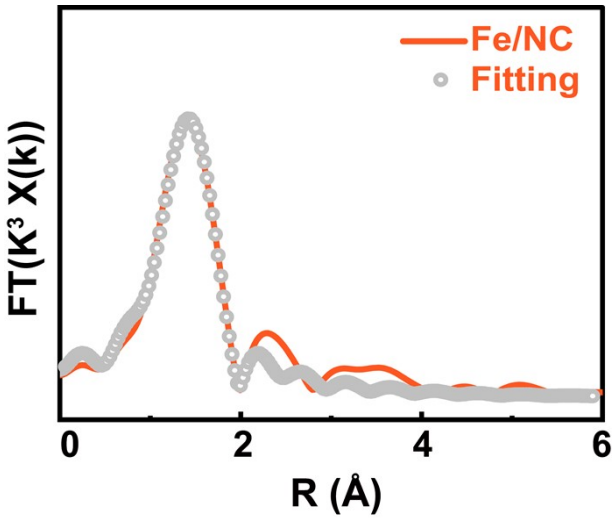

Fig. S6 FT-EXAFS fitting curves of Fe K-edge for Fe/NC.

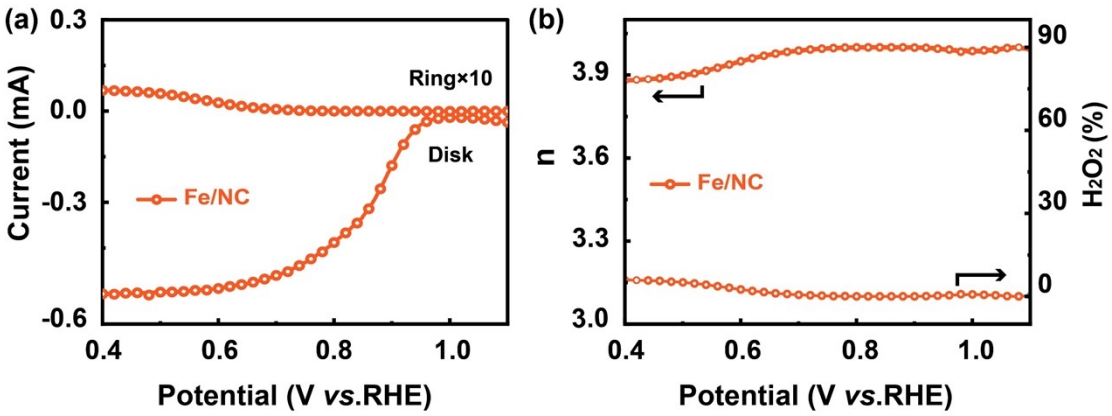

Fig. S7 (a) RRDE curves of Fe/NC and (b) H_2O_2 yield and electron-transfer number of Fe/NC.

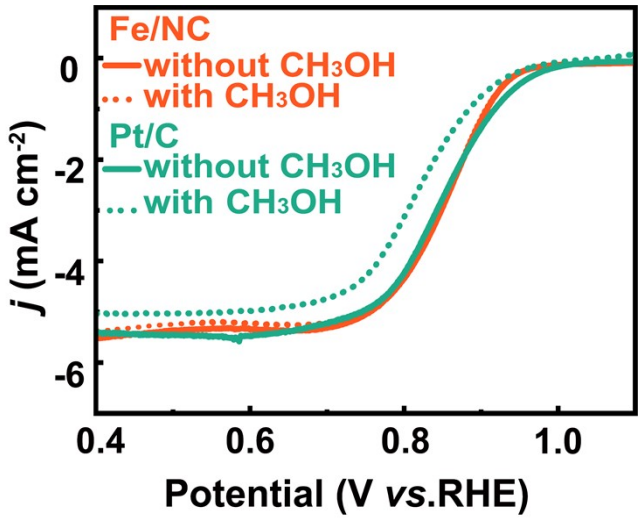

Fig. S8 LSV curves of catalysts against methanol.

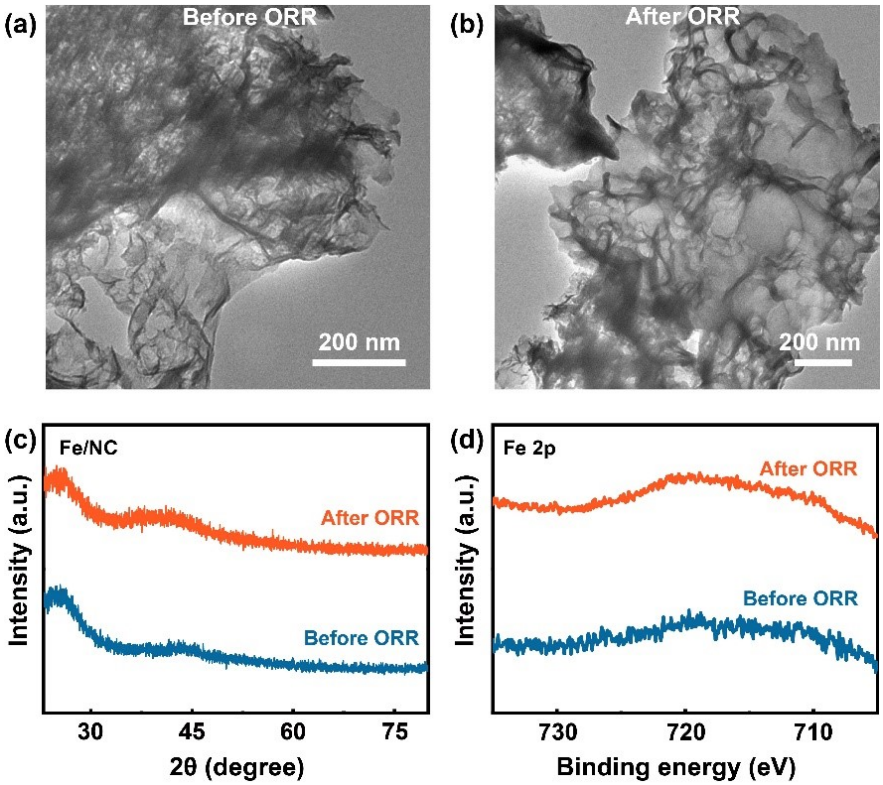

Fig. S9 Characterization of Fe/NC before and after the ORR reaction: (a, b) TEM images. (c) XRD pattern. (d) Fe 2p XPS spectra.

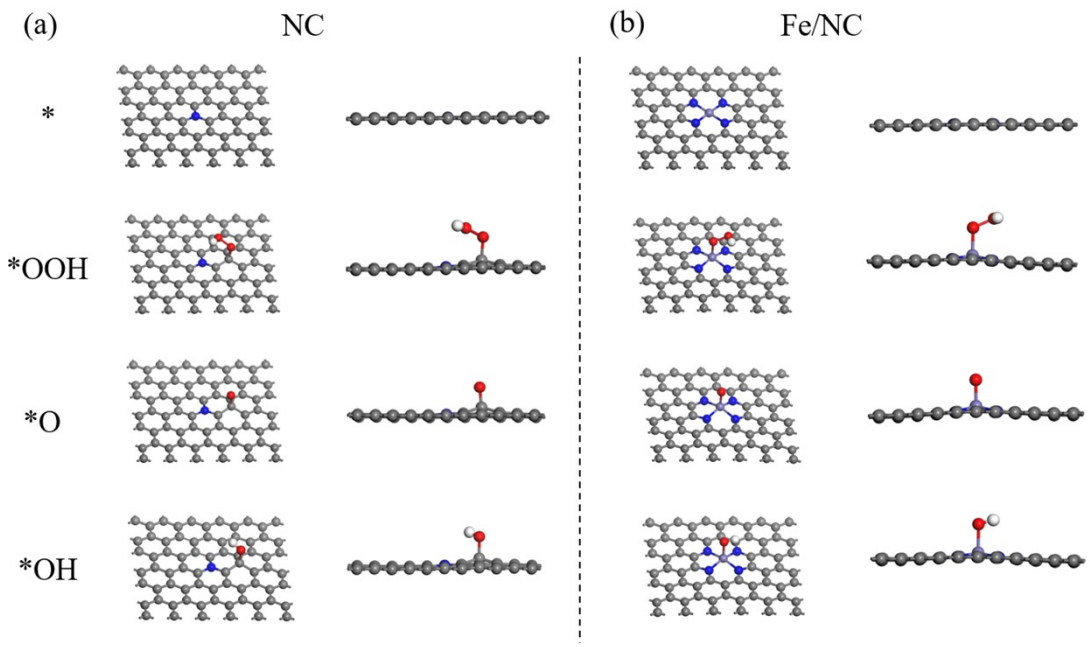

Fig. S10 Structures of ORR intermediates adsorbed on NC and Fe/NC.

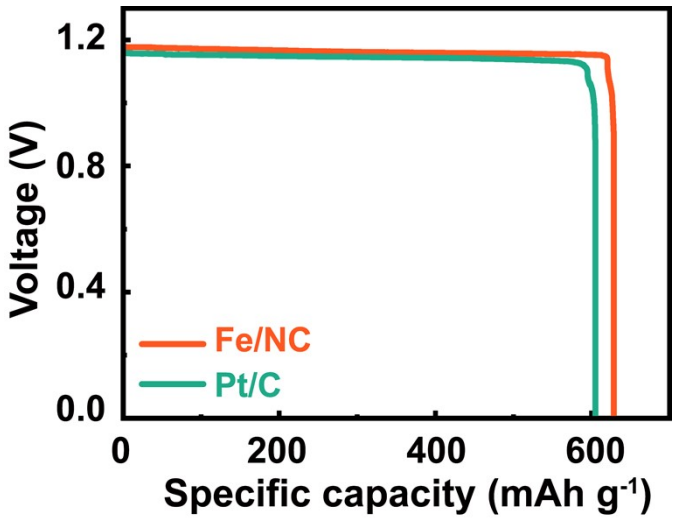

Fig. S11 Energy density curves of catalysts at 10 mA cm^{-2}.

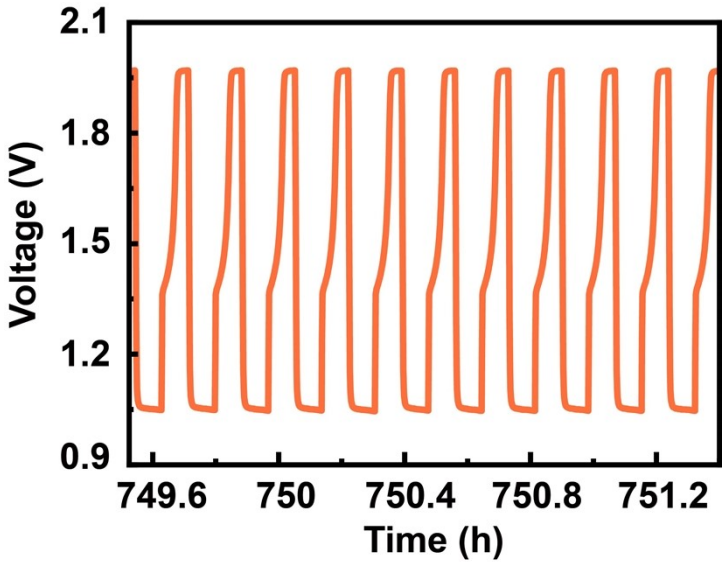

Fig. S12 A magnified region of a homemade liquid ZAB with Fe/NC at 10 mA cm^{-2}.

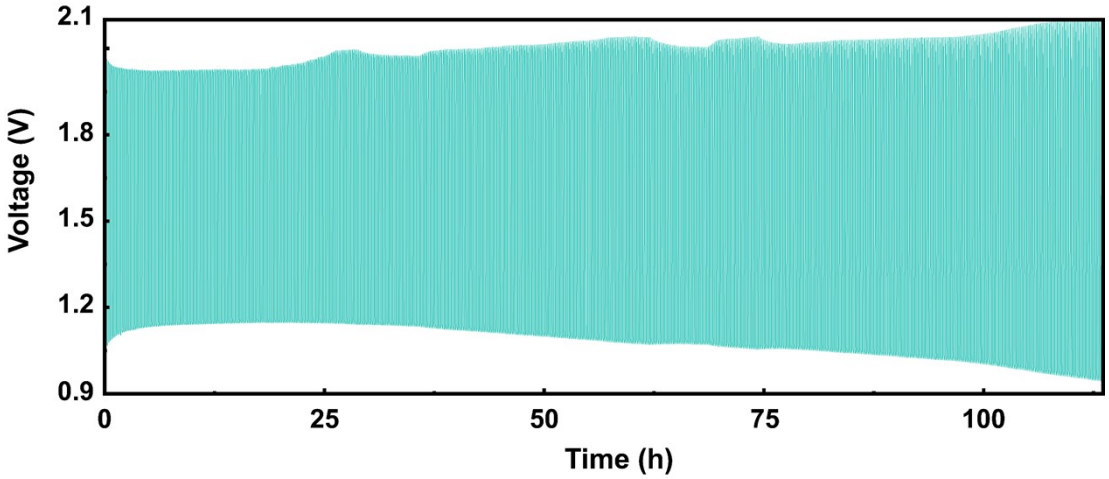

Fig. S13 Cycling stability of a home-made liquid ZAB with Pt/C at 10 mA cm^{-2}.

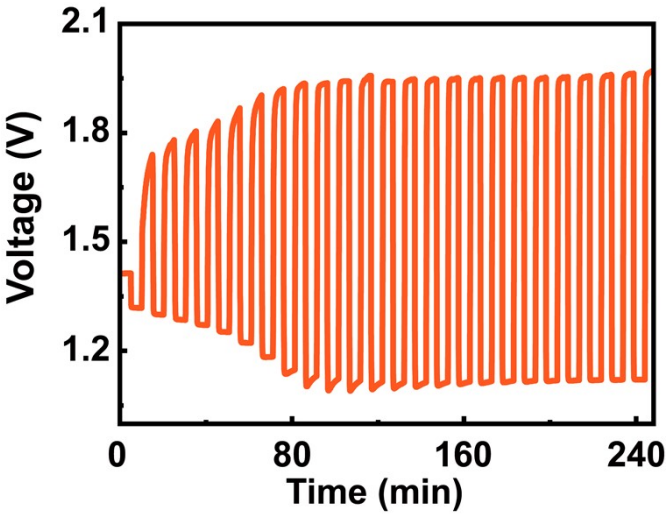

Fig. S14 Cycling stability of a coin-type ZAB with Fe/NC at 0.5 mA cm^{-2}.

Fig. S15 Digital photo of a LED powered by coin-type ZABs with Fe/NC.

Table S1. Structural parameters of Cu-Zn DA/HNC extracted from EXAFS fitting (S_0^2=0.75).

Scattering pair	CN	*R* (Å)	σ^2 (10^{-3}Å^2)	ΔE_0 (eV)	*R* factor
Fe-N (O)	5.2±1.3	1.98±0.02	10±4	2.9±2.8	0.001

S_0: the amplitude reduction factor; CN: the coordination number; *R*: interatomic distance; σ: debye-Waller factor; ΔE_0: edge-energy shift; *R* factor: the goodness of the fitting.

Table S2 Comparison of ORR activity of Fe/NC with that of reported catalysts in 0.1 M KOH.

Catalyst	$E_{1/2}$ (V vs. RHE)	Reference
Fe/NC	0.858	This work
Fe SAs@S/N-C	0.84	*J. Mater. Chem. A.*, 2024, ***12***, 11669-11680.
e-Fe_3C-NCT	0.85	*ACS Sustainable Chem. Eng.*, 2022, ***10***, 3346-3354.
FeCo-N-HCN	0.86	*Adv. Funct. Mater.*, 2021, ***31***, 2011289-2011301.
meso-Fe-N-C	0.846	*ACS Catal.*, 2020, ***11***, 74-81.
Fe_1-HNC-500-850	0.842	*Adv. Mater.*, 2020, ***32***, 1906905-1906912.
FC-C@NC	0.85	*Carbon Energy.*, 2020, ***2***, 283-293.
FeN_x@NC	0.842	*ACS Sustainable Chem. Eng.*, 2020, ***8***, 6979-6989.
FeNi/N-LCN	0.835	*Nano Lett.*, 2021, ***21***, 3098-3105.
Fe@FeSA-N-C-900	0.83	*J. Energy Chem.*, 2021, ***61***, 612-621.
mC-TpBpy-Fe	0.845	*Chem. Mater.*, 2019, ***31***, 3274-3280.
Fe_2O_3@NC-450	0.838	*J. Mater. Chem. A.*, 2020, ***8***, 25791-25804.
FeSA/N-PSCS	0.87	*Energy Storage Mater.*, 2023, ***59***, 102790-102800.
SAC-FeN-WPC	0.85	ACS Energy Lett. 2021, ***6***, 3624-3633.
FeNi-NPC-1000	0.867	*ACS Appl. Mater. Interfaces.,* 2024, ***16***, 12398-12406.
SA-FeCNS-800	0.85	*Chem. Eng. J.*, 2024, **484**, 149415-149427.
FeNi SAs/NC	0.84	*Adv. Energy Mater.*, 2021, ***11***, 2101242-2101250.
Ni-N_4/GHSs/Fe-N_4	0.83	*Adv. Mater.*, 2020, ***32***, 2003134-2003144.